Electronic Supplementary Material (ESI) for Catalysis Science & Technology.

Supplementary information

The nature of the active sites of Pd-Ga catalysts in the hydrogenation of CO_2 to methanol

Raydel Manrique[a,*], Jhonatan Rodríguez-Pereira[b], Sergio A. Rincón[c], Juan J. Bravo-Suárez[d,e], Víctor G. Baldovino-Medrano[b,c], Romel Jiménez[a,f], Alejandro Karelovic[a,f,g*]

[a] *Carbon and Catalysis Laboratory (CarboCat), Department of Chemical Engineering, Universidad de Concepción, Chile.*

[b] *Centro de Investigaciones en Catálisis, Escuela de Ingeniería Química, Universidad Industrial de Santander, Colombia.*

[c] *Laboratorio Central de Ciencia de Superficies, Universidad Industrial de Santander, Colombia.*

[d] *Chemical & Petroleum Engineering Department, The University of Kansas, Lawrence, KS, USA.*

[e] *Center for Environmentally Beneficial Catalysis, The University of Kansas, Lawrence, KS, USA.*

[f] *Unidad de Desarrollo Tecnológico (UDT), Universidad de Concepción, Chile.*

[g] *Millennium Nuclei on Catalytic Processes towards Sustainable Chemistry (CSC), Chile.*

**E-mail: rmanrique@udec.cl, akarelov@udec.cl*

S1 Mass and heat transfer limitations.

To obtain meaningful reaction rates, these must be measured in the absence of mass transport limitations or temperature gradients. There are experimental and theoretical methods to study the magnitude of transport processes in fixed-bed reactors and to verify if the measured rates are kinetically controlled. In this work, the equations proposed by Vannice[1] were used for this purpose.

S1.1 Intraparticle temperature gradients.

In order to corroborate the absence of thermal gradients during the catalytic tests, the Mears criterion was evaluated for the boundary condition in which the highest value in the expression would be obtained:

$$\frac{|\Delta H| r R_p^2}{\lambda T_s} < \frac{0.75 T_s R}{E_t} \qquad (S1)$$

This condition was analyzed for the catalytic test over Pd/Ga(1.0) catalyst, which has the highest TOF for the methanol synthesis at 280 °C and 8 bar.

$|\Delta H| = 49100\ J/mol$

$r = \frac{0.4\ \mu mol}{s * g_{cat}} = \frac{0.6\ mol}{s * m_{cat}^3}$ $(density\ SiO_2 = 2500 \frac{Kg}{m^3}, Bed\ porosity = 0.448)$

$R_p = 150\ \mu m$

$\lambda = 1.3 \frac{W}{K * m}$

$T_s = 280\ ^oC$

$R = 8.314 \frac{J}{mol * K}$

$E_t = 50000 \frac{J}{mol}$

Using Equation S1 it is verified that the inequality is established:

$9.2x10^{-7} < 6.9x10^{-2}$

This allows to conclude that the temperature gradients in this system are considered negligible.

S1.2 Intraparticle concentration gradients.

For the intraparticle mass transfer, the dimensionless Weisz-Prater number is calculated. It relates the reaction rate with respect to the diffusion in the pores of the particles. If the Weisz-

Prater number is less than or equal to 0.3, the internal diffusional limitations can be considered negligible:

$$\frac{r * R_p^2}{C_s * D_{eff}} \leq 0.3 \qquad (S2)$$

Besides, from the terms already defined here (C_s is the reagent concentration on the catalyst surface and D_{eff} is the effective diffusion coefficient), for the experiments of this work. The values are:

$$r = 0{,}6 \frac{mol}{s * m_{cat}^3}$$

$$R_p = 150\ \mu m$$

$$C_s = 44.1 \frac{mol}{m^3}$$

$$D_{eff} = 8{,}57x10^{-6} \frac{m^2}{s}$$

In this case the Weisz-Prater number is 3.5x10^{-6} which meets the criteria mentioned above.

S1.3 Interface concentration gradients.

In the case of gradients between the gas phase and the particle surface of the catalyst, an effectiveness factor (ψ) has been defined which relates the reaction rate measured with the reaction rate without diffusion limitations. The product of the effectiveness factor with the Dahmköhler number (Da_0) (which relates the reaction rate with the transport velocity of the fluid in the catalyst surface) is composed of observable quantities:

$$\psi * Da_0 = \frac{r}{K_g * a * C_s} \qquad (S3)$$

Where kg is the mass transfer coefficient between the fluid and the surface of catalyst particles, a is the area/volume ratio of catalyst particles and Cs the reagent concentration in the fluid.

$$r = 0.6 \frac{mol}{s * m_{cat}^3}$$

$$K_g = 0.04 \frac{m}{s}$$

$$a = 20000 \frac{m^2}{m^3}$$

$$C_s = 44.1\frac{mol}{m^3}$$

Consequently, the product $\psi * Da_0$ is equal to 1.7x10^{-6}, and ψ is approximately 1, which means that the limitations of external mass transfer are negligible.

Taking into account the previous results, it can be assumed that the reaction under study took place in a totally kinetic regime.

S2 Calculation of the turnover frequency for methanol and CO in the six catalysts sample.

S2.1 Palladium dispersion.

$$D_{Pd} = 6\frac{(V_m/a_m)}{d_p} \qquad (S4)$$

a_m: Area occupied by a single palladium atom on the crystalline surface (7,93 Å^2)^2.

V_m: Volume occupied by a single atom in the metal (14,7 Å^3)^2.

d_p: Mean particle diameter in nm (calculated by XRD).

S2.2 Formation rate of methanol and CO (mol product/mol Pd surface/s).

$$TOF = \frac{(r_p * M)}{(D_{Pd} * C_m)} \qquad (S5)$$

r_p: Production rate of methanol or CO (mol/s*$g_{catalyst}$).

M: Molecular weight of palladium (g/mol).

C_m: Pd mass fraction.

S3 Calculation of the approach to equilibrium.

The catalytic activity measurements were made based in the hydrogenation of CO_2 reactions, for the methanol production (1) and the formation of CO through the r-WGS (2).

$CO_2 + 3H_2 \leftrightarrows CH_3OH + H_2O$ (1)

$CO_2 + H_2 \leftrightarrows CO + H_2O$ (2)

The approach to equilibrium factor (η) allowed to define whether the catalytic tests were performed in a kinetic regime or in a thermodynamic regime. In addition, it was possible to

determine the forward rate for product formation. According to the reactions, the parameters η to be calculated correspond to the following:

$$\eta_1 = \frac{1}{K_{eq1}}\left(\frac{P_{CH3OH} * P_{H2O}}{P_{CO2} * P_{H2}^3}\right)$$

$$\eta_2 = \frac{1}{K_{eq2}}\left(\frac{P_{CO} * P_{H2O}}{P_{CO2} * P_{H2}}\right)$$

Where η_1 corresponds to the proximity to equilibrium for the synthesis of methanol and η_2 is the proximity to equilibrium for r-WGS.

The equilibrium concentrations for each component, if "a" and "b" correspond to the initial concentrations of CO_2 and H_2, respectively, are summarized in the table below:

Gas	**Experimental molar fraction [%] $yi \cdot 100$**
CO_2	a-(x+y)
H_2	b-(3x+y)
CH_3OH	x
CO	y
H_2O	x+y

As partial pressure is expressed as $Pi = yiP$, the equation of approach to equilibrium can be written as follows:

$$\eta_1 = \frac{1}{K_{eq1} * P^2}\left(\frac{y_{CH3OH} * y_{H2O}}{y_{CO2} * y_{H2}^3}\right)$$

$$\eta_2 = \frac{1}{K_{eq2}}\left(\frac{y_{CO} * y_{H2O}}{y_{CO2} * y_{H2}}\right)$$

The equilibrium constants were calculated according to van 't Hoff's equation:

$$ln\left(\frac{K_2}{K_1}\right) = \frac{\Delta H^{\circ}}{R}\left(\frac{1}{T_1} - \frac{1}{T_2}\right)$$

Where K_1 corresponds to the equilibrium constant under standard conditions and was determined by:

$$K_1 = exp(\frac{-\Delta G_{standard}}{R * T})$$

The standard $-\Delta G_{standard}$ for the methanol and CO formation reactions were determined from reported value[3].

The calculations led to the results shown below:

	Temperature (°C)			
Equilibrium constants	**280**	**260**	**240**	**220**
K_{eq} MeOH	9.17E-06	1.50E-05	2.49E-05	4.31E-05
K_{eq} r-WGS	1.85E-02	1.41E-02	9.16E-03	6.52E-03

	Temperature (°C)			
Approach to equilibrium factors	**280**	**260**	**240**	**220**
Pd				
η MeOH	2.20E-02	9.34E-03	2.75E-03	4.98E-04
η r-WGS	4.41E-02	2.22E-02	1.12E-02	3.90E-03
Pd/Ga(4.0)				
η MeOH	1.71E-03	2.36E-04	2.76E-05	5.39E-07
η r-WGS	8.89E-03	3.73E-03	1.79E-03	5.11E-04
Pd/Ga(2.0)				
η MeOH	1.02E-02	2.33E-03	3.54E-04	5.39E-05
η r-WGS	9.77E-02	3.79E-03	1.35E-03	5.15E-04
Pd/Ga(1.0)				
η MeOH	6.06E-01	1.99E-01	6.68E-02	1.93E-02
η r-WGS	1.55E-02	8.56E-03	4.73E-03	4.40E-03
Pd/Ga(0.5)				
η MeOH	9.13E-02	3.33E-02	8.32E-03	1.58E-03
η r-WGS	1.37E-03	6.75E-04	3.20E-04	1.26E-04
Pd/Ga(0.2)				
η MeOH	2.25E-03	8.25E-04	1.35E-04	2.49E-05
η r-WGS	2.03E-04	9.65E-05	3.50E-05	1.41E-05

The forward formation rates (r_f) are thus obtained from the net reaction rates (r_n) using the following equation:

$$r_f = \frac{r_n}{(1-\eta)}$$

Table S1. SiO_2 supported catalyst samples' nomenclature and their preparation conditions via incipient wet impregnation.

	Molar concentration (mol/L)				wt % metal	
Sample	$Pd(NO_3)_2$	$Ga(NO_3)_3$	$C_6H_{15}NO_3$	HNO_3	Pd	Ga
Pd/Ga(0.2)	0.4	2.0	9.6	0.8	4.5	15.1
Pd/Ga(0.5)	0.4	0.8	4.8	0.8	4.5	6.0
Pd/Ga(1.0)	0.4	0.4	3.2	0.8	4.5	2.9
Pd/Ga(2.0)	0.4	0.2	2.4	0.8	4.5	1.5
Pd/Ga(4.0)	0.4	0.1	2.0	0.8	4.5	0.7
Pd	0.4	--	1.6	0.8	4.5	--

Table S2. CO_2 conversion values over Pd, Pd/Ga(4.0), Pd/Ga(2.0), Pd/Ga(1.0), Pd/Ga(0.5), and Pd/Ga(0.2) catalysts. Temperature range 220-280 °C, 800 kPa, H_2/CO_2 = 3.

	CO_2 conversion (%)			
Sample	220 °C	240 °C	260 °C	280 °C
Pd/Ga(0.2)	0.25	0.46	0.92	1.47
Pd/Ga(0.5)	1.24	2.20	3.63	5.33
Pd/Ga(1.0)	4.62	6.96	11.14	21.7
Pd/Ga(2.0)	1.26	2.55	5.23	8.98
Pd/Ga(4.0)	1.27	2.44	5.05	9.36
Pd	3.03	6.08	10.97	19.20

Table S3. Average diameters of Pd metal particles determined by TEM.

Sample	Dp_{TEM} (nm)	$Dp_{TEM(S)}$ (nm)[a]	$Dp_{TEM(V)}$ (nm)[b]	Dp_{XRD} (nm)
Pd[a] (Pd/Ga(∞))	8±4[b]	12[c]	14	9
Pd/Ga(4.0)	12±5[b]	16[c]	18	13
Pd/Ga(2.0)	10±4[b]	13[c]	14	9
Pd/Ga(1.0)	15±9[b]	18[c]	21	15
Pd/Ga(0.5)	12±7[b]	21[c]	23	13
Pd/Ga(0.2)	27±6[b]	34[c]	36	18

[a] Surface-weighted average diameter $\sum_i n_i d_i^3 \Big/ \sum_i n_i d_i^2$

[b] Volume-weighted average diameter. $\sum_i n_i d_i^4 \Big/ \sum_i n_i d_i^3$

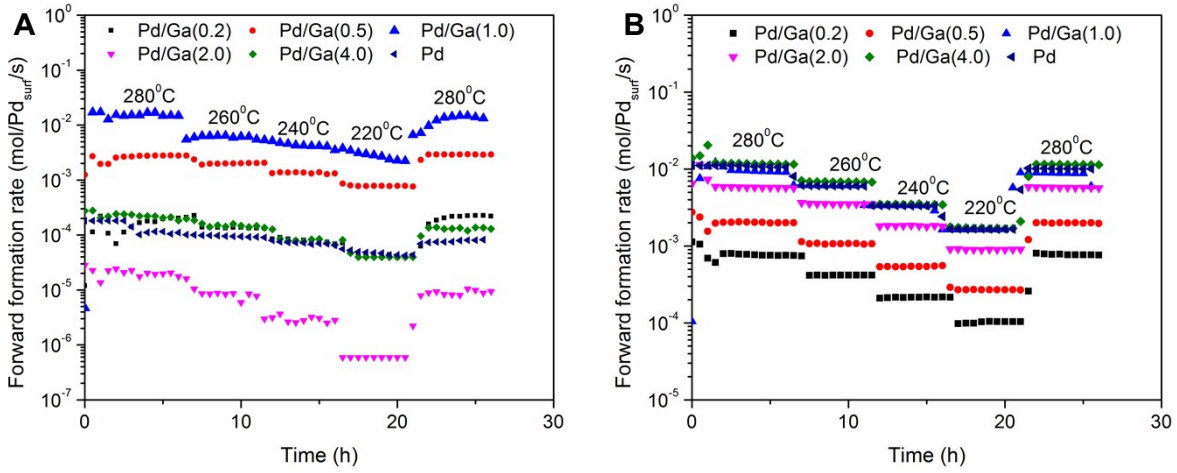

Figure S1. Intrinsic forward rate for the formation of methanol (A) and CO (B) as a function of reaction time. H_2/CO_2 = 3, P = 800 kPa.

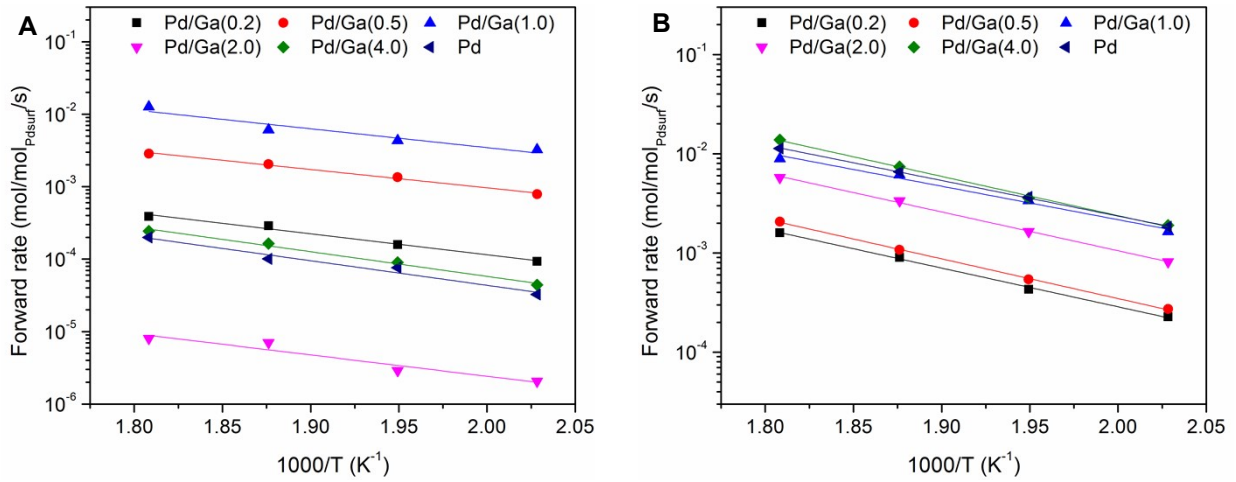

Figure S2. Arrhenius plot for the formation of (A) methanol and (B) CO. H_2/CO_2 = 3, P = 800 kPa, T = 220-280 °C.

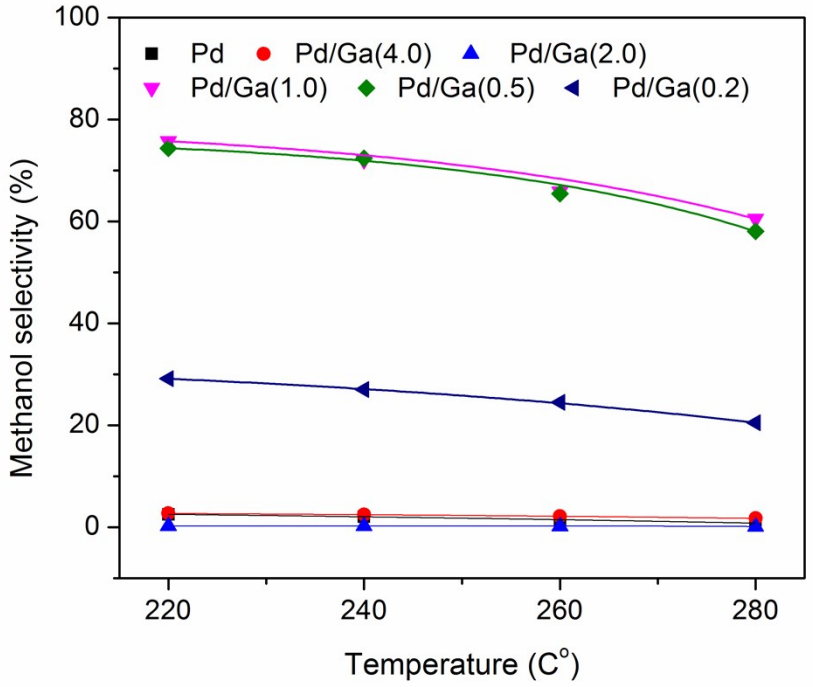

Figure S3. Selectivity to methanol as a function of temperature in the catalysts of Pd, Pd/Ga(4.0), Pd/Ga(2.0), Pd/Ga(1.0), Pd/Ga(0.5), Pd/Ga(0.2). H_2/CO_2 = 3, P = 800 kPa.

Pd/Ga(0.2)

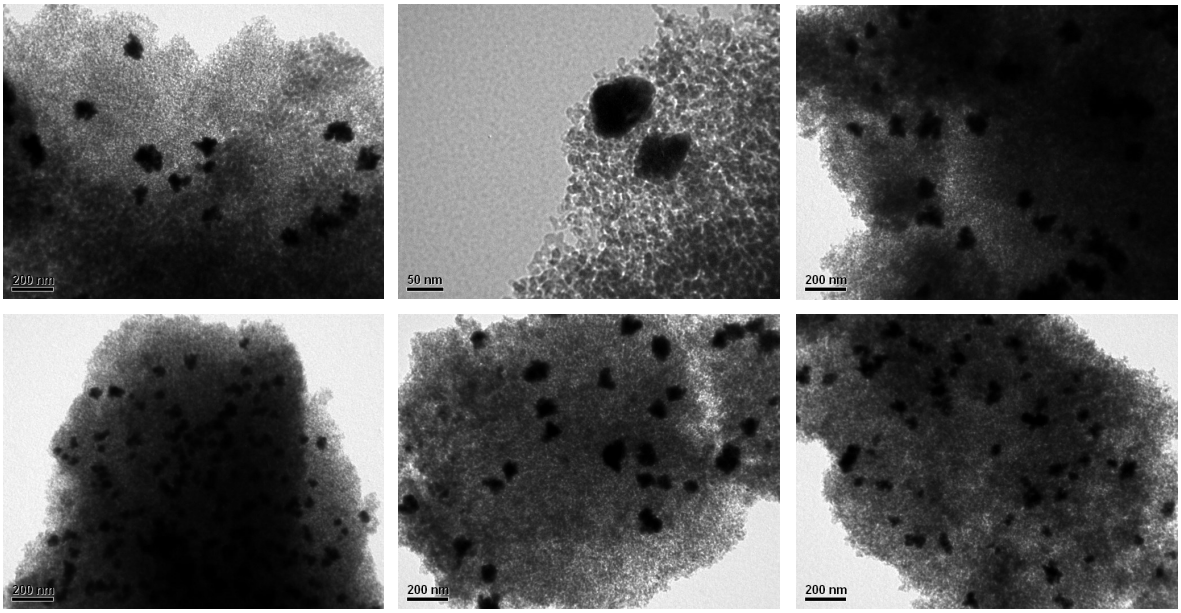

Figure S4. Transmission electron microscopy images for Pd/Ga(0.2), Pd/Ga(0.5), Pd/Ga(1.0), Pd/Ga(2.0), Pd/Ga(4.0), and Pd catalysts.

Pd/Ga(0.5)

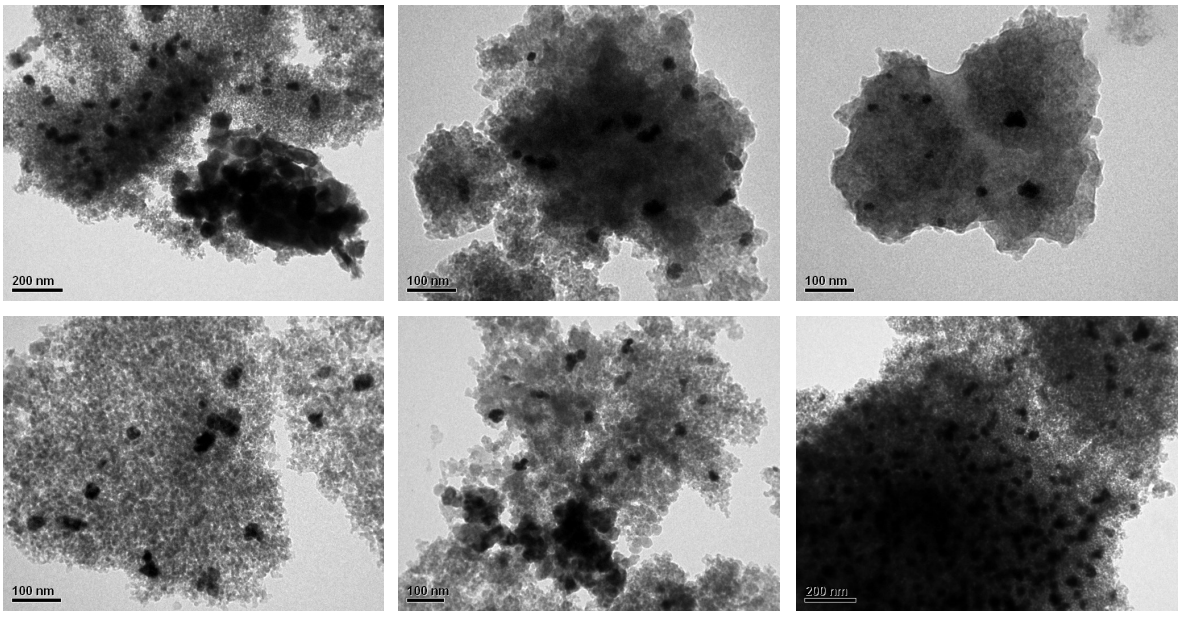

Pd/Ga(1.0)

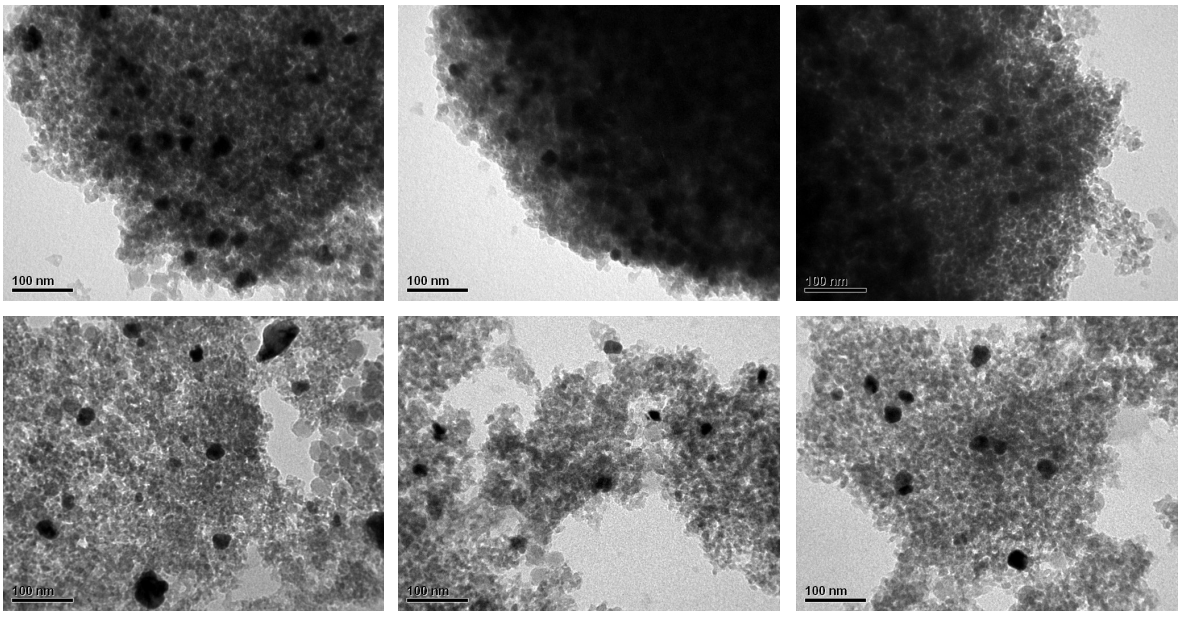

Figure S4 (continued). Transmission electron microscopy images for Pd/Ga(0.2), Pd/Ga(0.5), Pd/Ga(1.0), Pd/Ga(2.0), Pd/Ga(4.0), and Pd catalysts.

Pd/Ga(2.0)

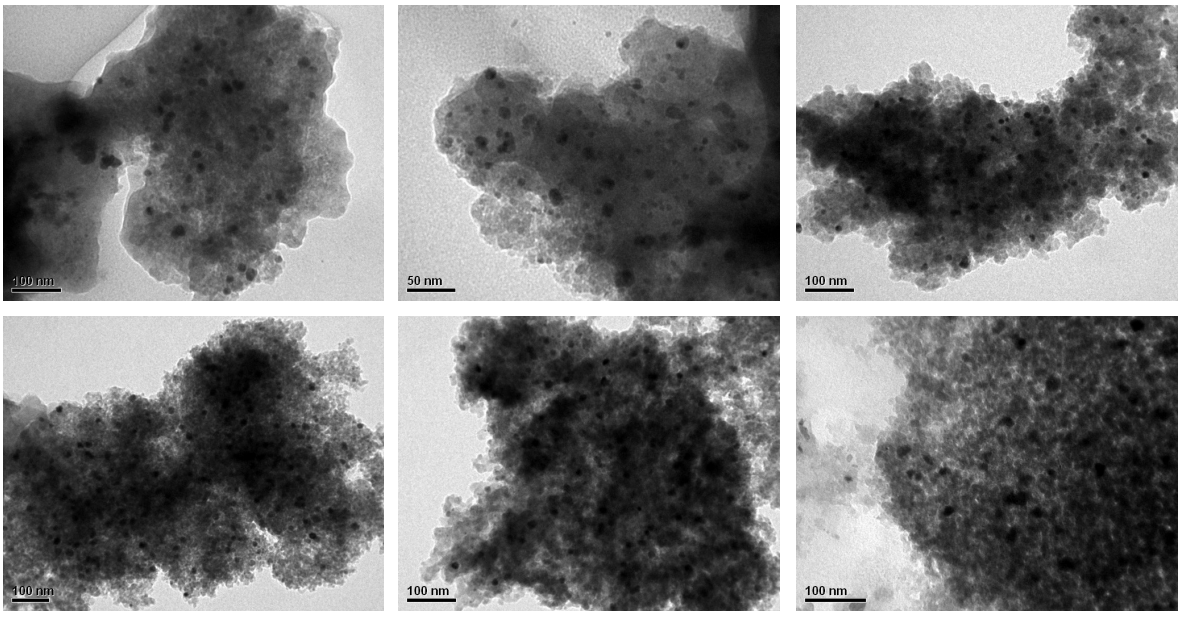

Pd/Ga(4.0)

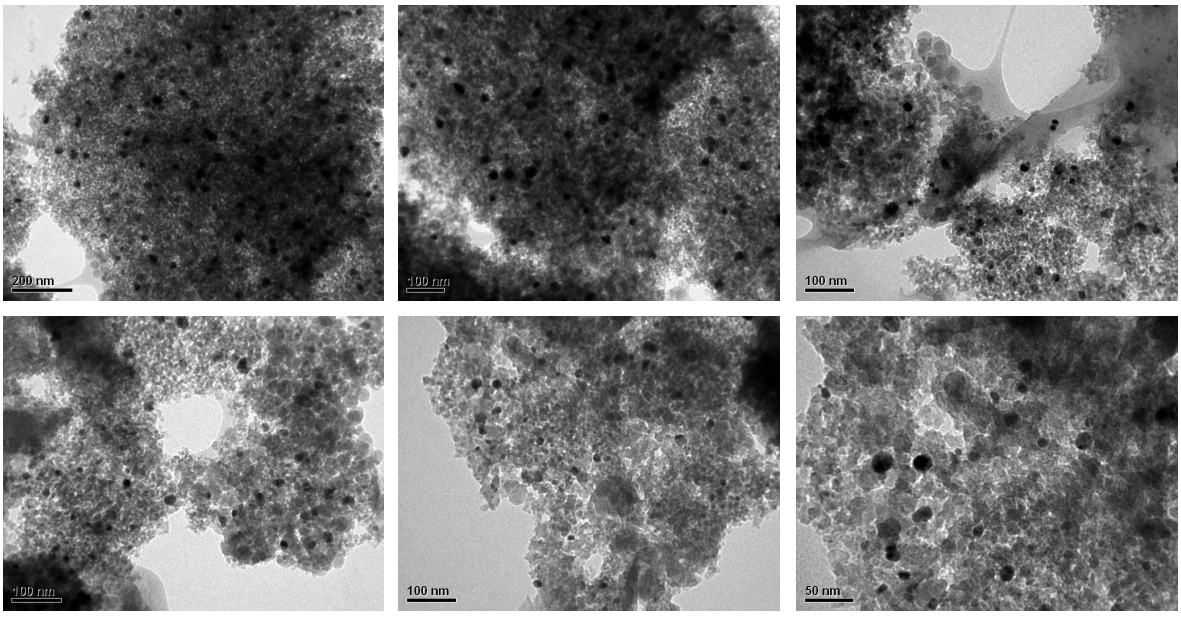

Figure S4 (continued). Transmission electron microscopy images for Pd/Ga(0.2), Pd/Ga(0.5), Pd/Ga(1.0), Pd/Ga(2.0), Pd/Ga(4.0), and Pd catalysts.

Pd

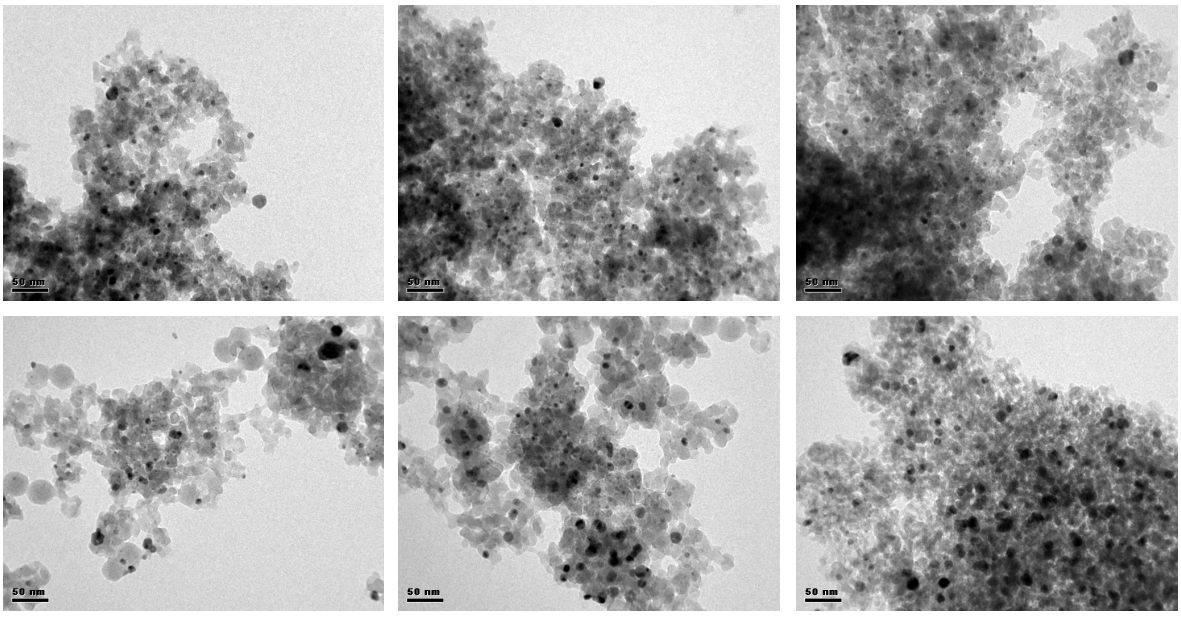

Figure S4 (continued). Transmission electron microscopy images for Pd/Ga(0.2), Pd/Ga(0.5), Pd/Ga(1.0), Pd/Ga(2.0), Pd/Ga(4.0), and Pd catalysts.

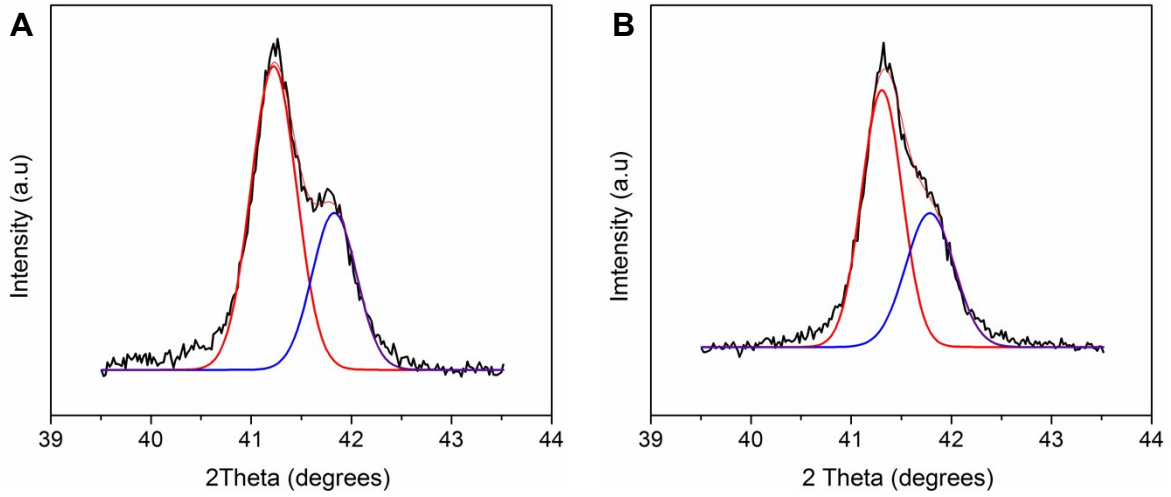

Figure S5. Results obtained from the deconvolution made to the peaks within the XRD patterns of A) Pd/Ga(0.5) and B) Pd/Ga(0.2). Software used: OriginPro 8.5.

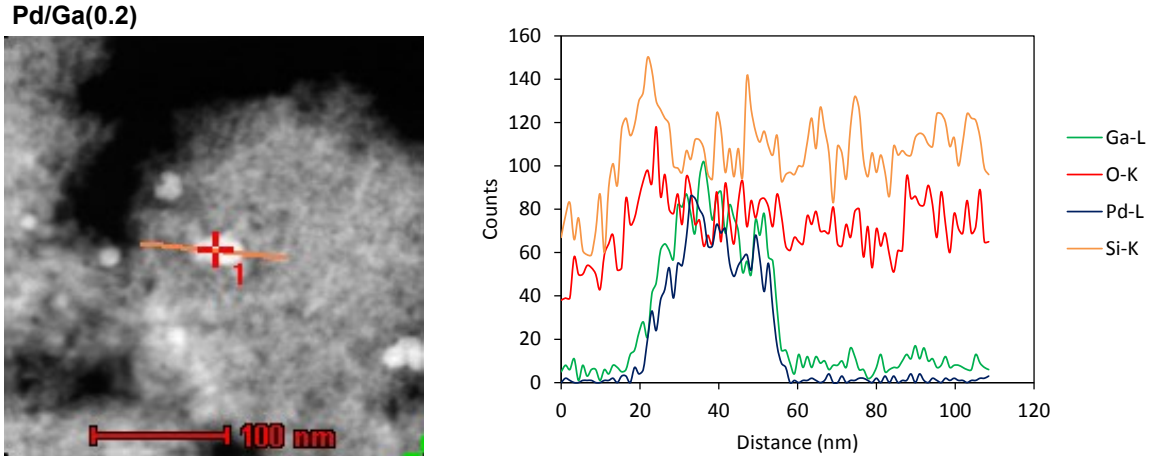

Figure S6. Linear scan analysis on the Pd/Ga(0.2) catalyst. TEM-EDS line spectra in the path indicated on selected metal particles.

Pd/Ga(4.0)

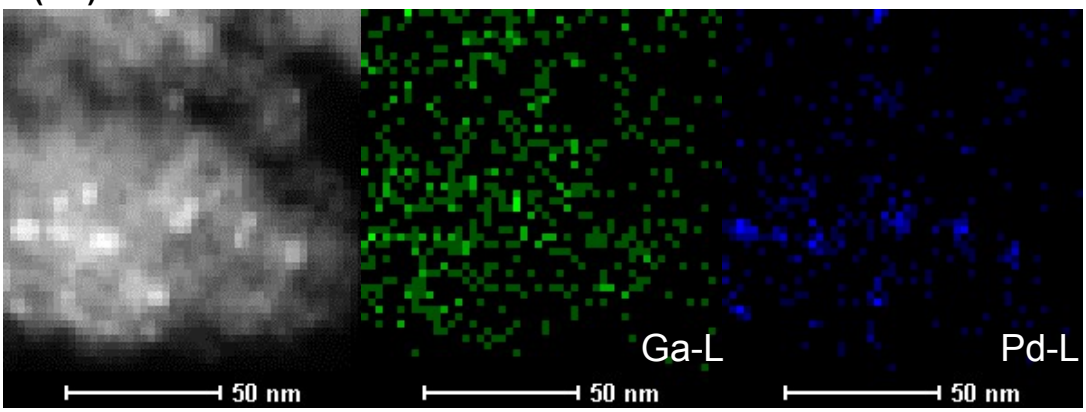

Pd/Ga(2.0)

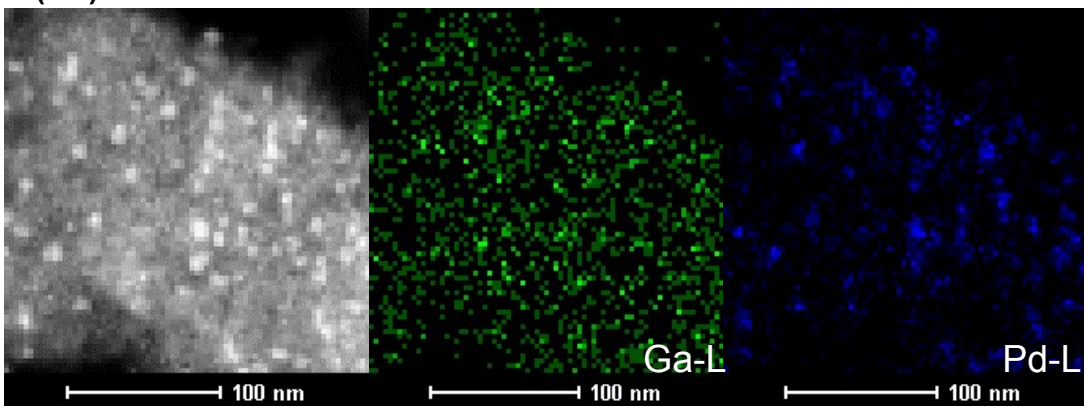

Figure S7. Transmission electron microscopy (STEM) images with energy dispersion X-ray spectroscopy (EDX) mapping for Pd/Ga(4.0), Pd/Ga(2.0), Pd/Ga(1.0), Pd/Ga(0.5), and Pd/Ga(0.2) catalysts.

Pd-Ga(1.0)/SiO_2

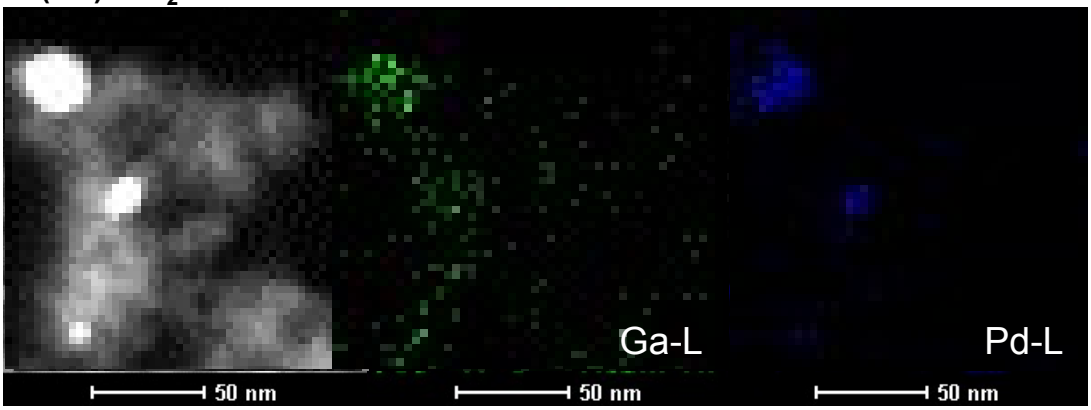

Pd/Ga(0.5)

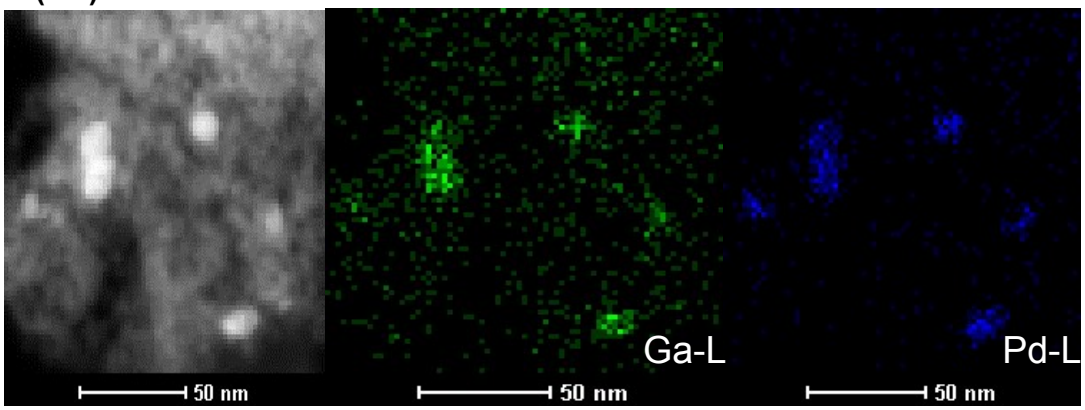

Pd/Ga(0.2)

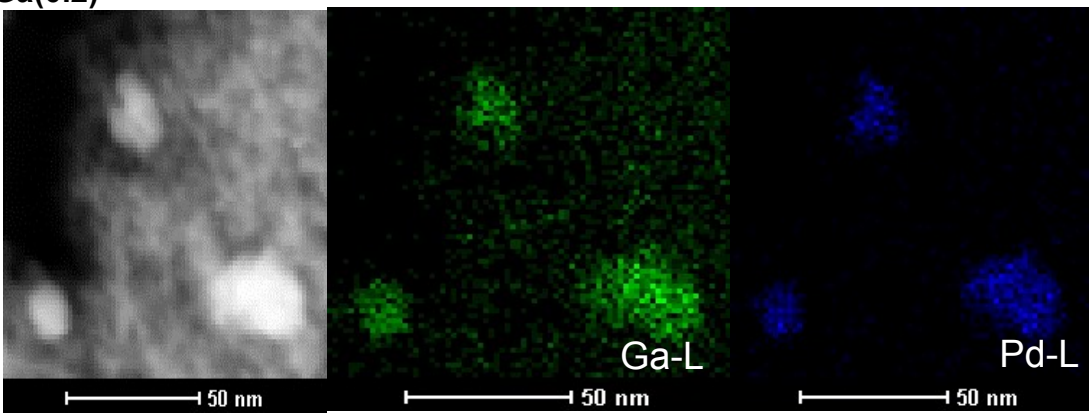

Figure S7 (continued). Transmission electron microscopy (STEM) images with energy dispersion X-ray spectroscopy (EDX) mapping for Pd/Ga(4.0), Pd/Ga(2.0), Pd/Ga(1.0), Pd/Ga(0.5), and Pd/Ga(0.2) catalysts.

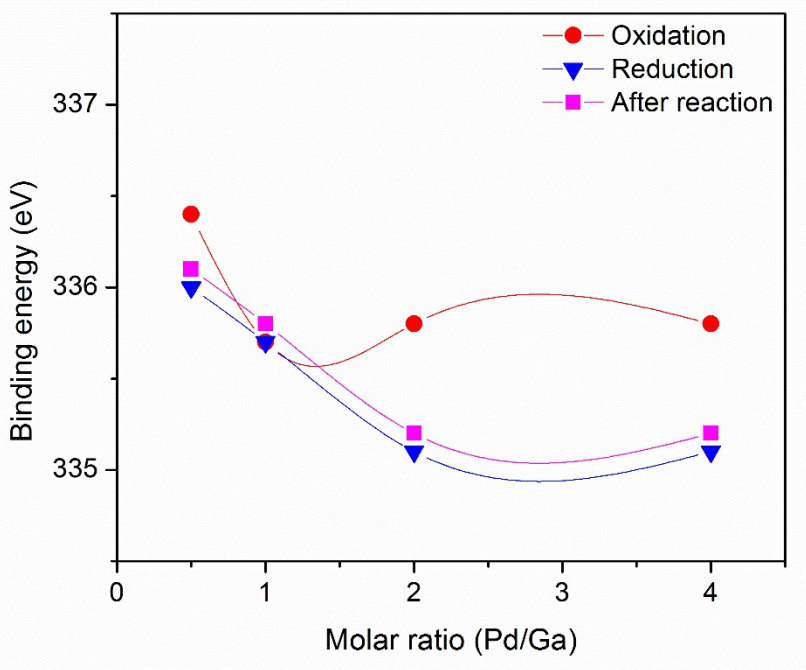

Figure S8. Variation of Pd $3d_{5/2}$ binding energy under different applied atmospheres with respect to the amount of Ga added for Pd/Ga(4.0), Pd/Ga(2.0), Pd/Ga(1.0), and Pd/Ga(0.5) catalysts.

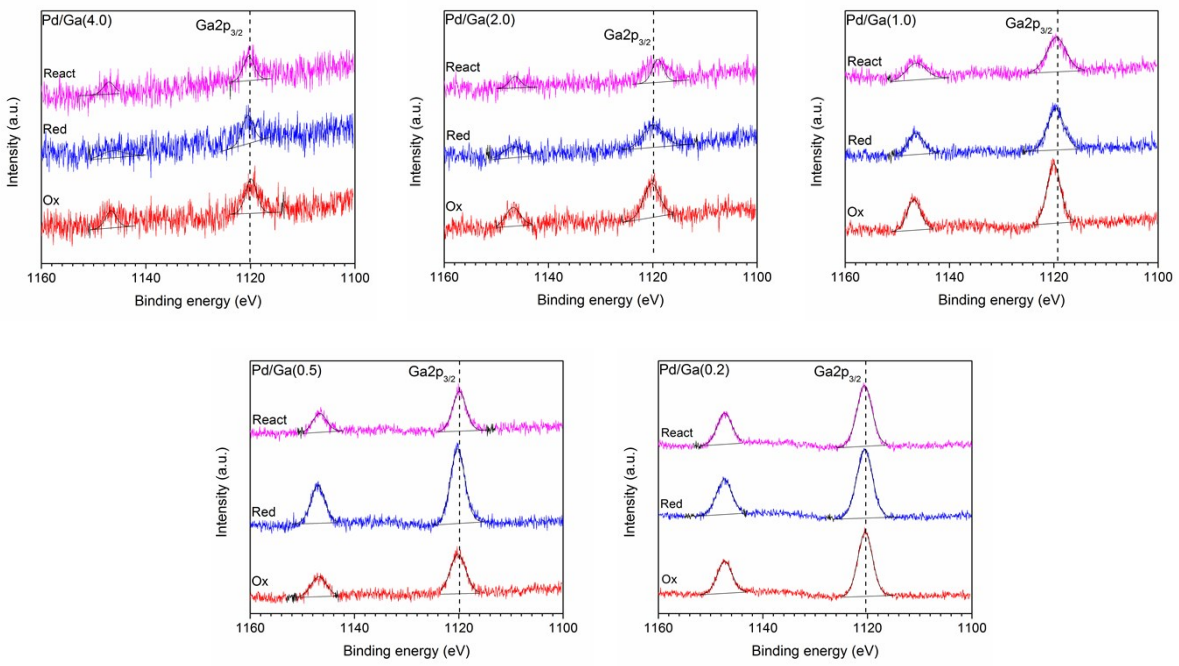

Figure S9. Ga 2p quasi in situ XPS results. Spectra recorded after different applied treatments. (Ox) oxygen flow (20 NTP cm^3/min, 101 kPa) at 25 °C; (Red) hydrogen flow (50 NTP cm^3/min, 101 kPa) at 500 °C; (React) reaction conditions at 260 °C (40 NTP cm^3/min, H_2/CO_2 = 3, 101 kPa).

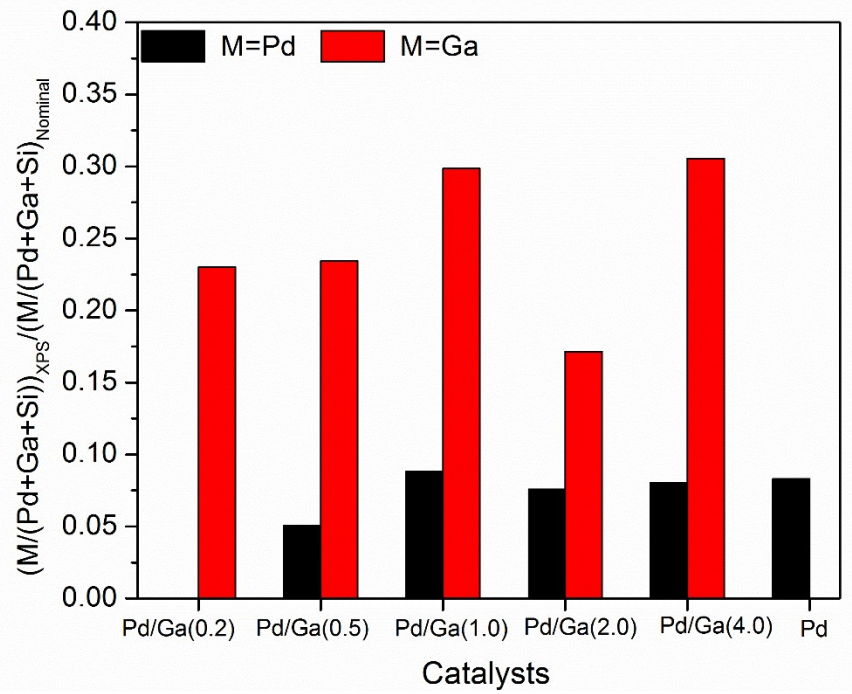

Figure S10. XPS ratio between the surface concentrations of Pd (or Ga) after reduction treatment determined by XPS and the nominal values. For Pd/Ga(0.2) catalyst, Pd concentration was below the detection limit.

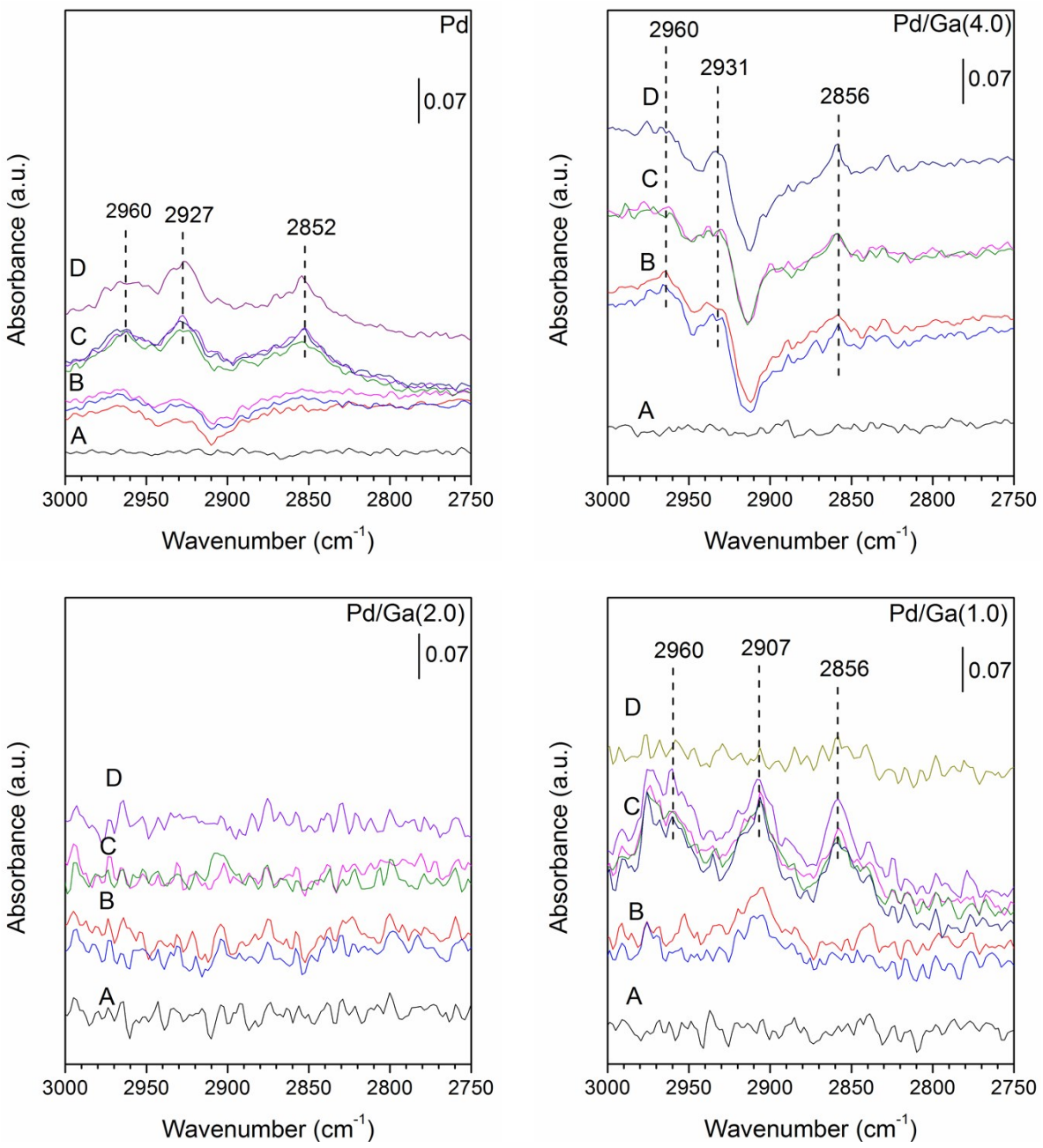

Figure S11. In situ DRIFTS spectra under different atmospheres for Pd, Pd/Ga(4.0), Pd/Ga(2.0), Pd/Ga(1.0), Pd/Ga(0.5), and Pd/Ga(0.2) catalysts. (A) Pretreatment in H_2 at 300 °C; (B) At reaction conditions of 240 °C (P = 101.3 kPa, H_2/CO_2 = 3); (C) At reaction conditions of 240 °C (P = 400 kPa, H_2/CO_2 = 3); (D) After 1 h in H_2 (21 NTP cm^3/min) at 240 °C (P = 400 kPa) following treatment C).

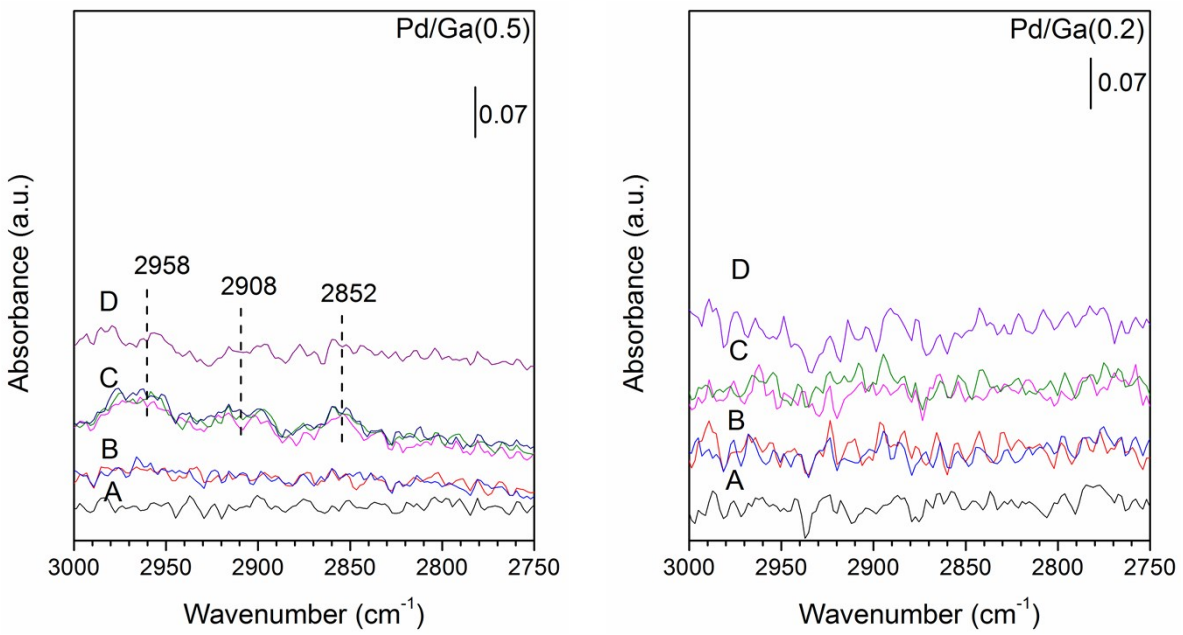

Figure S11 (continued). In situ DRIFTS spectra under different atmospheres for Pd, Pd/Ga(4.0), Pd/Ga(2.0), Pd/Ga(1.0), Pd/Ga(0.5), and Pd/Ga(0.2) catalysts. (A) Pretreatment in H_2 at 300 °C; (B) At reaction conditions of 240 °C (P = 101.3 kPa, H_2/CO_2 = 3); (C) At reaction conditions of 240 °C (P = 400 kPa, H_2/CO_2 = 3); (D) After 1 h in H_2 (21 NTP cm^3/min) at 240 °C (P = 400 kPa) following treatment C).

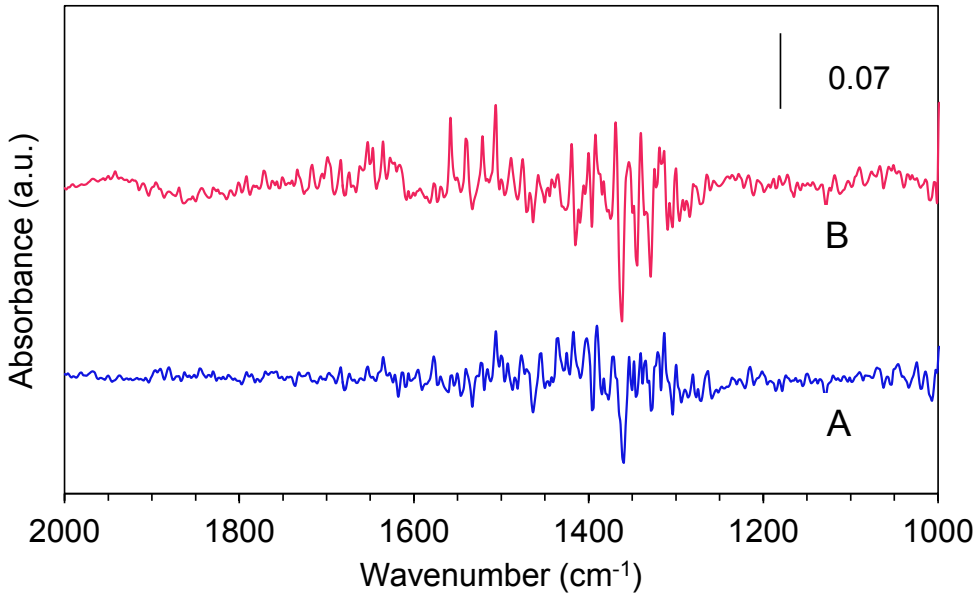

Figure S12. In situ DRIFTS spectra under different atmospheres for Pd/Ga(1.0) catalyst in the region 2000-1000 cm^{-1}. (A) Pretreatment in H_2 at 300 °C; (B) At reaction conditions of 240 °C (P = 400 kPa, H_2/CO_2 = 3).

References

1. M. A. Vannice, *Kinetics of catalytic reactions*, Springer, New York, 2005.

2. In *Handbook of Heterogeneous Catalysis*, pp. 1801–1900.

3. J. M. Smith, H. C. Van Ness and M. M. Abbott, *Introduction to chemical engineering thermodynamics*, McGraw-Hill, Boston, 7th edn., 2005.